

Breaking Boundaries: Balancing Performance and Robustness in Deep Wireless Traffic Forecasting

Romain Ilbert

University Paris-Cité & Huawei Paris Research Center
Paris, France
romain.ilbert@hotmail.fr

Zonghua Zhang

Huawei Paris Research Center
Paris, France
zonghua.zhang@huawei.com

ABSTRACT

Balancing the trade-off between accuracy and robustness is a long-standing challenge in time series forecasting. While most of existing robust algorithms have achieved certain suboptimal performance on clean data, sustaining the same performance level in the presence of data perturbations remains extremely hard. In this paper, we study a wide array of perturbation scenarios and propose novel defense mechanisms against adversarial attacks using real-world telecom data. We compare our strategy against two existing adversarial training algorithms under a range of maximal allowed perturbations, defined using ℓ_∞ -norm, $\epsilon \in [0.1, 0.4]$. Our findings reveal that our hybrid strategy, which is composed of a classifier to detect adversarial examples, a denoiser to eliminate noise from the perturbed data samples, and a standard forecaster, achieves the best performance on both clean and perturbed data. Our optimal model can retain up to 92.02% the performance of the original forecasting model in terms of Mean Squared Error (MSE) on clean data, while being more robust than the standard adversarially trained models on perturbed data. Its MSE is $2.71 \times$ and $2.51 \times$ lower than those of comparing methods on normal and perturbed data, respectively. In addition, the components of our models can be trained in parallel, resulting in better computational efficiency. Our results indicate that we can optimally balance the trade-off between the performance and robustness of forecasting models by improving the classifier and denoiser, even in the presence of sophisticated and destructive poisoning attacks.

CCS CONCEPTS

- Theory of computation → Models of learning; Adversary models;
- Networks → Wireless access points, base stations and infrastructure;
- General and reference → Reliability;
- Security and privacy → Mobile and wireless security.

Permission to make digital or hard copies of all or part of this work for personal or classroom use is granted without fee provided that copies are not made or distributed for profit or commercial advantage and that copies bear this notice and the full citation on the first page. Copyrights for components of this work owned by others than the author(s) must be honored. Abstracting with credit is permitted. To copy otherwise, or republish, to post on servers or to redistribute to lists, requires prior specific permission and/or a fee. Request permissions from permissions@acm.org.

ARTMAN '23, November 30, 2023, Copenhagen, Denmark

© 2023 Copyright held by the owner/author(s). Publication rights licensed to ACM. ACM ISBN 979-8-4007-0265-5/23/11...\$15.00
<https://doi.org/10.1145/3605772.3624002>

Thai V. Hoang

Huawei Paris Research Center
Paris, France
thai.v.hoang@huawei.com

Themis Palpanas

University of Paris
Paris, France
themis@mi.parisdescartes.fr

KEYWORDS

Forecasting, Poisoning, Classification, Denoising, Components, Robustness, Performance

ACM Reference Format:

Romain Ilbert, Thai V. Hoang, Zonghua Zhang, and Themis Palpanas. 2023. Breaking Boundaries: Balancing Performance and Robustness in Deep Wireless Traffic Forecasting. In *Proceedings of the 2023 Workshop on Recent Advances in Resilient and Trustworthy ML Systems in Autonomous Networks (ARTMAN '23), November 30, 2023, Copenhagen, Denmark*. ACM, New York, NY, USA, 12 pages. <https://doi.org/10.1145/3605772.3624002>

1 INTRODUCTION

Time series forecasting has been widely applied in various domains, such as finance, economics, healthcare, climate change, energy management, and telecommunications [19, 27, 30, 44, 68]. For example, wireless traffic forecasting has found its promising role in resource allocation, traffic engineering, and network security [2, 12, 21, 52, 59, 64]. In particular, one can obtain better load balancing and capacity planning by predicting future network traffic demand using historical data. Proactive maintenance and fault management can also be enabled by predicting network failures [9]. Recently, deep learning has been developed for time series forecasting, showing significant advantages over the classical methods in terms of performance, robustness, and generalizability [37, 50, 53, 62]. However, as those deep learning models applied in many other domains (e.g., Computer Vision, Natural Language Processing), whose performance and usability could be seriously undermined in the face of data poisoning attacks [7, 17, 24, 49, 58], the ones applied for time series forecasting are not immune from those attacks. One of the fundamental differences to be carefully considered is that time series data always exhibits temporal dependencies, thereby requiring special modeling techniques and attack strategies [10, 28, 31, 56].

Specifically, data poisoning refers to the attack that is intended to deliberately manipulate the data fed to a machine learning model [7], eventually undermining its performance. Data poisoning attack can be further classified into label flipping, data injection, and data modification [65], each of which has its own assumptions and requirements about the attacker's capabilities and goals [16]. For example, an attacker may have full or partial knowledge of the model architecture, access to the training data, or the ability to inject malicious samples into the dataset. Depending on the forecasting models and application scenarios, the consequence of a

poisoning attack can be extremely destructive. For instance, a successful poisoning attack to a financial forecasting model could lead to financial losses and market instability. In more critical scenarios like healthcare, where time series forecasting models are used for patient monitoring, disease diagnosis, and treatment planning, poisoning attacks can cause incorrect diagnoses, delayed treatments, and even life-threatening situations [40, 54]. Similarly, poisoned wireless traffic forecasting models could result in deteriorated network performance and even network failures [42]. As a matter of fact, all these attacks have been demonstrated to be effective in various domains, such as Computer Vision (CV), Natural Language Processing (NLP) [6, 34, 48]. But their feasibility and effectiveness in time series forecasting have been studied much less than they deserve [38, 39, 71]. In addition, the thread models in most of the existing works are oversimplified, while the concern is limited to the trade-off between model's performance and robustness. Taking wireless traffic prediction as a specific scenario, we make the following contributions in this paper:

- A comprehensive examination of data poisoning attacks on deep learning-based time series forecasting models.
- A novel defense mechanism against these attacks that involves one classifier to identify perturbed data and one denoiser to remove perturbations from those data.
- A new bi-level masking attack strategy under extreme adversarial conditions, with ℓ_∞ -norm $\rightarrow 0.4$ across all sequences and their individual steps.
- Our optimal model preserves up to 92.02% of the original forecasting model's MSE on clean data. Its MSE is up to 2.71 \times and 2.51 \times lower than those of existing methods on clean and perturbed data, respectively.

The effectiveness of our proposed defense mechanism has been validated on real-world telecom dataset. Experimental results show that it can significantly improve the performance of wireless traffic prediction models, even under strong poisoning attacks, while maintaining its performance on clean data.

The rest of this paper is organized as follows. Section II reviews related work on wireless traffic prediction and adversarial attacks. Section III and IV presents in detail the proposed attack and defense mechanisms, respectively. Section V describes the experimental setup and presents the evaluation results. Finally, Section VI concludes the paper with discussions and future research directions.

2 RELATED WORK

We review in this section existing works that are closely related to ours. This includes time series prediction, data poisoning attacks and the corresponding countermeasures.

2.1 Wireless Traffic Prediction

Wireless traffic prediction has been extensively studied due to its importance in various network applications. So far, various techniques have been proposed to model and forecast wireless traffic effectively. Traditional forecasting methods for time series, such as ARIMA models, exponential smoothing state-space models, and STL, are frequently utilized to model linear relationships, trends, and seasonality in data [10, 15, 20, 32]. Despite their widespread use, these methods exhibit certain limitations. In particular, they

may falter when dealing with highly nonlinear or intricate patterns and often necessitate manual parameter tuning, a process that can be laborious and may not guarantee optimal performance.

To address these limitations, deep learning models have emerged as popular choices for time series forecasting tasks. Recurrent Neural Networks (RNN), Long Short-Term Memory networks (LSTM), and Gated Recurrent Units (GRU) have been particularly successful in capturing complex temporal dependencies and nonlinear relationships in time series data [18, 29]. These models can automatically learn intricate patterns, often resulting in improved predictive performance compared to traditional methods. More recently, Convolutional Neural Networks (CNN) showed promising results in capturing local and global patterns in time series data [3, 8]. Transformer-based architectures, which were initially designed for NLP tasks, have also been adapted for time series forecasting [61]. Considering the application scenario and characteristics of the used dataset, we choose LSTM for the implementation of the baseline forecaster in this work.

2.2 Data Poisoning Attacks

To date, several types of attacks have been identified in the literature. For example, an attacker can alter the labels (i.e., label flipping) of a subset of training data [65], or introduce malicious samples (i.e., data injection) into the training dataset [57], and even subtly alter existing data points (i.e., data modification) to mislead the forecasting task during training [7]. In order to achieve these attacks, an adversary should possess particular capabilities and goals, such as the knowledge about model's architecture, and the access privileges to training data [16]. For example, Projected Gradient Descent (PGD) aims at identifying the most effective adversarial examples by maximizing the model's loss function through iteratively perturbing input samples [35, 41]. To successfully perform PGD, an adversary needs access to the model's architecture, the ability to compute the loss function and its gradient with respect to the input data. This type of attack is considered as strong adversary, as it can craft adversarial examples that are more likely to fool the model than single-step methods such as Fast Gradient Sign Method (FGSM) [24].

2.3 Countermeasures against Poisoning Attacks

Defending against data poisoning attacks remains a challenging and active area of research in recent years. To date, various defense strategies have been proposed to mitigate the effects of data poisoning attacks, and they can be classified into two categories. The first relies on data sanitization by filtering out perturbed samples from the training data. For example, in [5, 36, 51], the authors illustrated that outlier detection techniques can be used to identify and remove potentially poisoned samples. However, a recent study has provided a theoretical framework and pointed out that detecting adversarial examples (i.e., poisoned data) is nearly as hard as classifying them [60].

Other than data sanitization, we have also seen some attempts to learning robust machine learning models, which are expected to be less sensitive to the presence of poisoned data than their normal counterparts [23, 47, 57].

In particular, adversarial training has recently shown significant promise and gained popularity for improving the robustness of machine learning models. Its key idea is to train models on adversarially perturbed examples in order to force it to generalize better under adversarial conditions [41]. A number of strategies have been developed in [22, 43, 66] following this idea. For example, in [69], an approach termed TRADES was developed to balance the trade-off between the standard and robust accuracy. It is also worth mentioning that a recent study investigated the limits of adversarial training against norm-bounded adversarial examples and provided insights into the potential trade-offs between standard and robust generalization [26].

As mentioned previously in Section 2.2, despite tremendous efforts paid to the development of countermeasures against poisoning attacks in CV and NLP, much less work has focused on time series analytics, in particular scenarios such as speech recognition [33] and industrial control systems [13]. Our work focuses on learning robust forecasting models for the wireless network traffic prediction problem. It can be considered as a new contribution to the aforementioned second category. Unlike [60], we demonstrate that guaranteeing robustness against adversarial attacks is as hard as classifying and denoising the adversarial samples.

2.4 Comparison to Previous Works

In order to distinguish our contributions from existing works, we enumerate below the four models that have been implemented for performance benchmarking in this work. Details of these models are presented in Fig. 2.

- M_1 : a forecaster trained with normal data;
- M_2 : a forecaster trained with normal and poisoned data;
- M_3 : a hybrid model composed of a classifier to identify and a denoiser to remove perturbation from poisoned data ahead of a forecaster;
- M_4 : a hybrid model composed of a classifier to identify and direct normal and poisoned data to two separated forecasters.

The forecasters employed in these models use LSTM networks and share the same architecture. It can be seen that M_1 serves as a baseline forecasting model. M_2 embodies the approach of Madry et al.'s [41], which is usually used as the adversarially trained baseline forecasting model. To the best of our knowledge, no existing work has ever incorporated a classifier and/or a denoiser into an end-to-end adversarially training framework as our proposed M_3 and M_4 models. In particular, the authors of [71] employ a data sanitization approach and a statistical-based anomaly detection method to remove potential outliers.

3 THREAT MODELING

Poisoning attacks in wireless traffic prediction have been formulated as machine learning problems in both centralized and distributed scenarios [71]. In this work, we focus on centralized settings, due to their wide-spread implementation and application in real-world scenarios. In such a setting, the traffic data of different clients are transferred to a common server in order to train a global forecasting model using a standard model optimization process.

Let's consider F_1 , a forecaster trained on normal data using a standard empirical risk minimization (ERM) scheme. It is defined as

$f_1(x; \theta)$, where x is the input data and θ represents F_1 's parameters. The loss function \mathcal{L} used in the training is defined as the MSE between the predicted $f_1(x_i; \theta)$ and actual values y_i . $\hat{\theta}^*$ is defined as the set of parameters in Θ that minimizes \mathcal{L} over p sequences x_i with labels y_i in our training dataset:

$$\hat{\theta}^* = \underset{\theta \in \Theta}{\operatorname{argmin}} \frac{1}{p} \sum_{i=1}^p \mathcal{L}(f_1(x_i; \theta), y_i) \quad (1)$$

We assume that an adversary has the ability to introduce perturbations to any point in the historical data of any client. Formally, we denote the i -th batch of historical data as $X_i = [x_1, \dots, x_m]_i^T \in \mathbb{R}^{m \times n}$, which is composed of m univariate sequences of length n , and the corresponding future values as $Y_i = [y_1, \dots, y_m]_i^T \in \mathbb{R}^m$. $\delta_i \in \mathbb{R}^{m \times n}$ is the perturbation applied to X_i . For each batch i , the aim is to find an optimal perturbation δ_i^* that maximizes the loss \mathcal{L} defined in Eq. 2. The perturbation to each sequence x is limited within a ℓ_∞ -norm ball of radius ϵ : $\mathcal{B}_\infty(x, \epsilon) = \{x' \in \mathbb{R}^n : \|x' - x\|_\infty \leq \epsilon\}$. $\epsilon = 0.3$ means 30% of the range of the traffic volume in the training set, where range is defined as the difference between the maximum and minimum traffic volume. If X_i is a batch of normal data, $X_i + \delta_i$ is the corresponding batch of perturbed data. Finding the optimal perturbation $\delta_i^* \in \Delta = \mathcal{B}_\infty(x_i, \epsilon)^m \in \mathbb{R}^{m \times n}$ for each batch X_i reduces to solving the following optimization problem:

$$\delta_i^* = \underset{\delta_i \in \Delta}{\operatorname{argmax}} \mathcal{L}(f_1(X_i + \delta_i; \theta), Y_i) \quad (2)$$

Here, we assume that the adversary's goal is to perturb the target forecasting model by poisoning historical data [14]. With the ability to target any base station and manipulate any subsequence data, these attacks can be pervasive and difficult to be detected. In general, the forecaster F_1 can be attacked in various ways. We choose a popular attack called Projected Gradient Descent (PGD) due to its widespread adoption in adversarial machine learning [11, 39, 70].

3.1 PGD Attack

To approximate a solution for Eq. 2 and find the optimal disturbance that maximizes MSE of F_1 , we use a PGD attack, as shown in Eq. 3. This attack employs a projection for T steps, a learning rate α and an initial perturbation $\delta_{i,0} = 0$ or $\delta_{i,0} \sim \text{Uniform}(-\epsilon, +\epsilon)$. This approximation ultimately allows us to presume that $\delta_i^* \approx \delta_{i,T}$. For notation purposes, we use $\tilde{X}_{i,t}$ to represent the perturbed batch X_i at step t with a perturbation $\delta_{i,t}$, i.e. $\tilde{X}_{i,t} = X_i + \delta_{i,t}$, with an initial perturbed batch $X_{i,0} = [x_{i,0}, \dots, x_{m,0}]_i^T$ as shown in Eq. 4.

$$\tilde{X}_{i,t+1} \leftarrow \operatorname{Proj}_\Delta \left(\tilde{X}_{i,t} + \alpha \cdot \operatorname{sign} \left(\nabla_{\tilde{X}_{i,t}} \mathcal{L}(f(\tilde{X}_{i,t}; \theta), Y_i) \right) \right) \quad (3)$$

$$X_{i,0} = X_i + \mathbb{1}(\delta_{i,0} \sim \text{Uniform}(-\epsilon, +\epsilon)) \cdot \delta_{i,0} \quad (4)$$

At each step, a new perturbed batch is crafted using the direction of the loss gradient with respect to the previous perturbed batch. The magnitude of the perturbation is bounded by the radius ϵ of an ℓ_∞ -norm ball centered on the initial input $X_{i,0}$ as illustrated in Eq. 4. The radius ϵ signifies the maximum permissible perturbation on the input, serving a pivotal role in our adversarial training setup. Each component illustrated in Figure 1 has its unique ϵ value: ϵ_d for the denoiser D , ϵ_f for the forecaster F_2 , ϵ_c for the classifier C , and ϵ_t during the testing phase.

In order to distinguish perturbed batches from non-perturbed ones, the classifier may require fine-tuning to endure smaller adversarial perturbations, thus a smaller ϵ_c . On the contrary, a larger ϵ_f is essential to demonstrate robustness against substantial adversarial perturbations. We employ a PGD attack that computes a projection within a ball of radius $\epsilon_f \geq \epsilon_c$ for the first $T - 1$ steps as detailed in Eqs. 5 and 6. At the final step T , the attack yields two outputs (Eqs. 7 and 8): one adversarial training batch for the forecaster F_2 within the ϵ_f radius ball and another for the classifier within the ϵ_c radius ball. Since $\epsilon_f \geq \epsilon_t$, we project into the ϵ_f radius ball during the first $T - 1$ steps. This strategy allows the perturbation to traverse a larger space before projecting into a ϵ_c radius ball, thus potentially capturing more information. For this reason, Δ depends on t , the projection step, so that $\Delta = \Delta_t$. We provide more information about the form of Δ_t in the following equations :

$$\forall t \in \llbracket 1, T - 1 \rrbracket : \Delta_t = \bigtimes_{i=1}^m \mathcal{B}_{\infty}(x_{i,0}, \epsilon_f) \quad (5)$$

$$\forall t \in \llbracket 1, T - 1 \rrbracket : \text{Proj}_{\Delta_{t+1}}(v) = \text{Clamp}(v, x - \epsilon_f, x + \epsilon_f) \quad (6)$$

$$\Delta_T = \Delta_T^f \times \Delta_T^c = \bigtimes_{i=1}^m \mathcal{B}_{\infty}(x_{i,0}, \epsilon_f) \times \bigtimes_{i=1}^m \mathcal{B}_{\infty}(x_{i,0}, \epsilon_c) \quad (7)$$

$$\text{Proj}_{\Delta_T}(v) = \begin{bmatrix} \text{Clamp}(v, x - \epsilon_f, x + \epsilon_f) \\ \text{Clamp}(v, x - \epsilon_c, x + \epsilon_c) \end{bmatrix}^T \quad (8)$$

Unlike the formulation in Madry et al. [41], F_2 in our work serves as a surrogate version of F_1 . F_1 is attacked by PGD and aids in generating the poisoned samples, on which F_2 is trained on. There is no parameter sharing between F_1 and F_2 , but they share the same network architecture. Both use two LSTM layers coupled with layer normalization and dropout, a fully connected layer, terminates with sigmoid activation function. Our approach enhances the attack, since if the adversarial training and the PGD attack are performed on the same forecaster as in [41], it naturally becomes more resistant to these attacks during training. Therefore, attacking it becomes more complicated, which could prevent the attack from being optimal and not reaching the boundary of the ball of radius ϵ . Here, we attack F_1 , which has no defense mechanism, ensuring the PGD attack retains its effectiveness throughout training. During the testing phase, the attacker injects noise within a ℓ_{∞} -norm ball of radius ϵ_t .

3.2 Perturbed Sequences

Previous works usually assume that when a client (i.e., a base station) is compromised, the entire historical sequence from that client is perturbed [39]. In this work, we assume that the attacker can manipulate the value of individual time steps of each sequence from each client in order to evade detection.

To accommodate this scenario, we generate partially perturbed sequences by applying various masks to the original sequences. Differing from Zheng et al. [71] who perturb entire sequences, our method operates at a bi-level granularity. We use two hyperparameters $\%pseq$ to control the proportion of sequences and k to determine the number of individual time-steps to perturb. This perturbation strategy adds an extra layer of complexity and specificity in our attacks.

As an example for a sequence of length $n = 3$, the mask $q = (0, 0, 1)$ modifies the last value of a given sequence in the normal batch X_i and replace it by its perturbed version, i.e., the last value of this corresponding sequence in $\tilde{X}_{i,T}$. For notations, we introduce \mathbb{Q}_n as the set of different masks of length n . $|\mathbb{Q}_n| = 2^n$ for the classifier that uses both perturbed and unperturbed data, and $|\mathbb{Q}_n| = 2^n - 1$ for the denoiser and forecaster F_2 that use perturbed examples only, without the non-perturbation mask $(0, 0, 0)$. Each mask q is a binary sequence that can be drawn uniformly from \mathbb{Q}_n to perturb sequences in the batch. Applying this mask implies replacing a value in a sequence by its perturbed version if and only if the mask at the corresponding position takes a value 1. The final masked, perturbed batch takes the form $X_i + q \odot \delta_{i,T}$, as illustrated in Eq. 9. We utilize the Hadamard product, denoted by \odot , such that $q \odot A$ corresponds to the element-wise multiplication of each row of A by each element of q , resulting in a matrix of the same shape as A .

$$(\mathbb{1}_n - q) \odot X_i + q \odot \tilde{X}_{i,T} = X_i + q \odot \delta_{i,T} \quad (9)$$

3.3 Attacker Capabilities and Knowledge

While previous works assume that the adversaries have limited knowledge and abilities, we assume in this work that an attacker is very familiar with wireless traffic forecasting systems and can manipulate the data at will. In particular, this adversary can target any, and possibly multiple, base stations and individual data points using a $T = 10$ -steps PGD attack with the following knowledge:

- The adversary needs to know the targeted forecaster, including its architecture and the associated weights, biases, and loss function. This is because a PGD attack involves tweaking the input data to make the forecaster perform poorly, which requires understanding how it works.
- The adversary needs to know about the data used to train the targeted forecaster. This is because a PGD attack involves creating misleading examples based on the training data to trick the forecaster.

The assumed capabilities allow us to have a robustness analysis under the most challenging conditions, i.e., adversary has complete information as that of defender, which is known as a white box attack. One may argue that such a sophisticated attack may not be feasible in reality.

We, however, take this “worst-case scenario” as a stress test for any vulnerable deep forecasting model. In other words, if a model can withstand an attack by such a well-equipped attacker, its robustness and resilience could be sufficiently validated.

It is worth noting that the novelty of our proposed attack lies in the adversary’s ability to manipulate numerous base stations, potentially simultaneously, at time steps of their choice. This significantly amplifies the potential strength of the attack compared to those previous attacks studied in the field, such as the attacks against Bayesian forecasting dynamic models [46], and the targeted attacks to time series forecasting models [25]. Similarly, the attacks on multivariate probabilistic forecasting models reported in [39] did not consider manipulating numerous base stations at chosen time steps. By considering a more powerful adversary, we extend the previous studies about the robustness of deep forecasting models under more sophisticated attack scenarios, which will benefit the design of more resilient wireless network prediction systems.

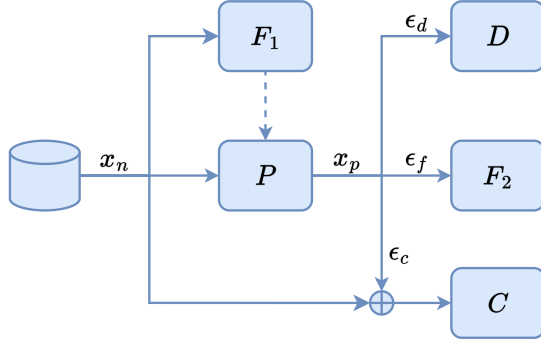


Figure 1: Four components trained separately: F_1 is the forecaster trained only on normal samples x_n and used for PGD attack P , which produces adversarial samples x_p . The classifier C is trained on a mix of normal and poisoned samples, whereas the denoiser D and the forecaster F_2 are trained on adversarial samples only.

4 DEFENSE MECHANISMS

To cope with the given attacks, we develop our defense mechanisms in a systematic approach by leveraging and integrating the components in Fig. 1. These defense mechanisms, called models M_i , are shown in Fig. 2. In particular, we include two baseline models M_1 and M_2 for the comparison purpose. As shown in the figure, M_1 and M_2 make use of the two forecasters F_1 (trained with normal samples) and F_2 (trained with 100% poisoned samples). M_3 is composed of classifier C that detects adversarial samples and denoiser D that removes perturbation from the detected adversarial samples, along with forecaster F_1 . In doing so, we transform the problem of model's performance and robustness to adversarial attacks into adversarial example classification and feature denoising, breaking the traditional trade-off between model robustness and accuracy. M_4 uses classifier C with forecaster F_1 if the C considers the sequence as normal, or with forecaster F_2 otherwise. In our approach, the components F_1 , F_2 , C , and D are trained in an independent manner from one another. Thanks to this structure, the performance of individual components does not have an impact on each other. It is also computationally efficient since components can be trained in parallel.

4.1 Adversarial Training

Adversarial training, a method for bolstering machine learning models against adversarial attacks, involves training on a blend of clean and perturbed examples to ensure model performance even when the instances are manipulated by an adversary[41, 63, 72]. This approach can be computationally costly and requires a trade-off between accuracy on clean and adversarial examples. To mitigate these issues, recent work embeds adversarial perturbations into the neural network's parameter space [63], while alternative methods such as label smoothing and logit squeezing mimic adversarial training mechanisms [55].

The mathematical distinction between Empirical Risk Minimization (ERM) and Adversarial Risk Minimization (ARM) lies in their objective functions. In particular, ERM minimizes empirical loss

over the data distribution (Eq. 10), optimizing for average-case performance, while ARM minimizes the maximum loss over all possible perturbations δ within a set Δ (Eq. 11), optimizing for worst-case performance. This makes ARM more computationally demanding than ERM, as it requires solving an additional optimization problem for each subsequence in order to find the loss-maximizing perturbation δ .

$$\hat{\mathcal{R}}(\theta) = \frac{1}{m} \sum_{i=1}^m \mathcal{L}(f(X_i; \theta), Y_i) \quad (10)$$

$$\hat{\mathcal{R}}_{\text{adv}}(\theta) = \frac{1}{m} \sum_{i=1}^m \max_{\delta_i \in \Delta} \mathcal{L}(f(X_i + q \odot \delta_i; \theta), Y_i) \quad (11)$$

Fig. 1 which shows that the two forecasters F_1 and F_2 share identical architectures but differ in their training regimens. Specifically, F_1 undergoes standard training and serves as the target for a PGD attack to generate adversarial examples, which are then utilized to train the counterpart component, F_2 . The unique aspect of F_2 is its training on adversarial data, aiming to enhance its robustness against such attacks. It plays a crucial role in our defense model M_4 , providing prediction of poisoned sequence predicted by the classifier C . Similarly, the M_3 model is using adversarial examples through C and D trainings.

It is worth noting here that despite its architectural similarity to F_1 , F_2 requires an extended training period to converge due to the adversarial nature of its training (100% perturbed samples are used for training). This extended training period is necessary for enhanced robustness against significant perturbations.

4.2 Classification of Adversarial Examples

The purpose of classification of adversarial examples in time series data is to identify whether a given sequence has been perturbed or not. This can be essentially treated as a traditional anomaly detection problem, which aims at pinpointing anomalous sequences in their entirety [1, 45, 67]. While anomaly detection flags deviations from normal behavior, adversarial examples entail stealthily crafted perturbations to deceive the target models.

In our methodology, we adopt a balanced training regimen for C , e.g., 50% normal sequences and 50% perturbed sequences with norm value ϵ_c in each batch (Fig. 1). The classifier has binary output: 0 for unperturbed sequences and 1 for sequences with at least one perturbed time step.

C employs a series of Inception modules, each composed of 1D convolutions with kernel sizes of 1 and 3 and padding equal to 0 and 1 respectively. Following each Inception module, batch normalization is performed, followed by ReLU activation and dropout. Afterward, Global Average Pooling is conducted before a final fully connected layer. The loss is computed using cross-entropy.

By classifying each sub-sequence, our aim is to detect even the most subtle perturbations within the time series data. Even if only a single time step is perturbed, we flag the entire sequence as adversarial. This approach poses a unique challenge for classification, as it demands the detection of perturbed sequences even when the perturbation is minimal. However, this heightened sensitivity to minor perturbations enhances our system's detection capabilities, thereby fortifying the defense mechanism against sophisticated adversarial attacks.

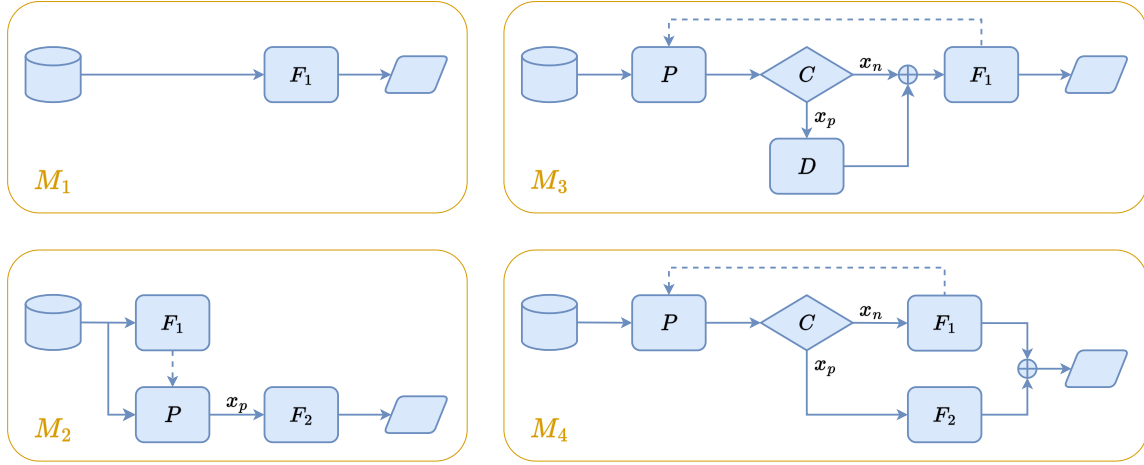


Figure 2: The four models and their composing components presented in Fig. 1. M_1 and M_2 employ forecasters F_1 and F_2 . M_3 utilizes classifier C (adversarial sample detector) and denoiser D (if perturbation detected), followed by forecaster F_1 . M_4 uses classifier C with F_2 (if perturbation detected), or with F_1 otherwise. x_n and x_p represent normal and perturbed sequences, respectively.

4.3 Denoising Poisoned Data

The denoiser is designed to remove poisoned samples and make the sequences clean. It undergoes training with entirely noisy sequences with norm value $\epsilon_d = \epsilon_f$, with labels mirroring these sequences without noise (Fig. 1). Within the M_3 model, the denoiser serves to expunge noise from sequences flagged as noisy by the classifier, as depicted in Fig. 2. Following the denoiser's application, the normal forecaster F_1 is employed, considering the denoiser's output sequences as normal.

This component is pivotal in maintaining the integrity of the base data within the training dataset. In the event of new data being disturbed, the denoiser can be employed to remove the noise. This ensures that the original training dataset remains free of noisy data.

The Denoiser D employs a basic auto-encoder architecture. The encoder part uses a linear layer, batch normalization, ReLU activation, and dropout, followed by a decoder that mirrors the same structure. It employs MSE as its loss function.

5 EXPERIMENTAL EVALUATION

5.1 Dataset Description

In our time series forecasting study, we use the Telecom Italia dataset [4] as a comprehensive source of information. Specifically, we focus on call volumes in Milan's urban environment. This dataset provides a rich and detailed source of information, allowing us to delve deep into the patterns and trends of telecommunications usage. To align with a prior study by Zheng et al. [71], in our research, we choose 100 base stations using a consistent random seed. These base stations provide a broad and representative sample of the telecommunications activity in the city. Our study is analyzing hourly data over an 8-week period, 7 of which are used for training and 1 for testing. In order to predict time t , we divide the univariate time series for each base station into sub-sequences of length 3 ($t - 1$, $t - 2$, and $t - 24$ hours). This approach allows us to capture

the temporal dependencies in the data, which is crucial for accurate forecasting. However, defending against adversarial attacks is particularly challenging due to the dataset's high standard deviation, with an average standard deviation of 0.26 after 0-1 normalization. This high-level variation in the data makes it difficult to distinguish normal fluctuations from adversarial perturbations, presenting a significant challenge in our defense against adversarial attacks.

5.2 Component Updates

In our study, we adopt a unique approach for training that strikes a balance between computational efficiency and stability of updates. Specifically, we iterate over the batches within each epoch, compute the gradients for each batch, but only update the component's parameters after each epoch. This method is akin to batch gradient descent with a batch size equal to the size of our dataset, and it offers at least two advantages,

- This method ensures that each update is based on a comprehensive view of the data, reducing the influence of outliers and noise on the learning process, thereby enhancing the stability of our updates. By aggregating the gradients over the entire dataset before performing an update, we mitigate the risk of erratic component behavior that can arise from the high variance in our data.
- It is computationally efficient. While benefiting from the granularity of batch-wise gradient computation, it avoids the computational cost of frequent backpropagation steps associated with updating the component parameters after each batch.

In particular, F_1 , F_2 , C and D are trained independently, each epoch of which involves processing batches with a length 512.

5.3 Evaluation Metrics

Our objective is to have the MSE of our hybrid models M_3 and M_4 as close as possible to the MSE of our standard model M_1 on unperturbed data. We can consider one hypothetical scenario with two models, M_1 and M_3 . Let's imagine that initially, M_1 performs better than M_3 on standard, unperturbed data, with an MSE of 1.5 versus 2. However, when we introduce data perturbations, the narrative can shift significantly. M_3 might show remarkable resilience to these data perturbations, maintaining, for instance, 90.9% (e.g., an increase from 2 to 2.2 MSE) of its original performance level, indicating its superior adaptability to challenging conditions. Conversely, M_1 's performance could deteriorate dramatically, only retaining around 33% (an increase from 1.5 to 4.5 MSE) of its original effectiveness. This example emphasizes that even if a model seems slightly less effective on clean data, its ability to retain a high percentage of its original performance in the face of real-world perturbations could make it the preferred choice for handling unpredictable data scenarios.

In addition to evaluating the robustness of our models based on their MSE, we are also interested in the accuracy of C in detecting adversarial examples, as it provides insight into how challenging it is for the system to identify these intentionally misleading data points. We examine this metric under various parameters and consider how it changes with different levels of data perturbation. By analyzing the classifier's accuracy in this way, we can gain a more comprehensive understanding of our system's resilience to adversarial attacks and identify potential areas for improvement.

5.4 Experimental Setup

Our setup involves historical data with a length $n = 3$. Each time step in the subsequence can either be perturbed or not, leading to one normal version and 7 possible perturbed versions. This approach is more comprehensive than other methods that perturb the entire sequence [41, 63, 72]. By using this perturbation approach, we can gain a better understanding of the potential vulnerabilities of our forecasting F_1 and train a more robust adversarial forecaster F_2 . This is because we consider a wider range of attacks, compared to fully perturbed sequences.

5.4.1 Components. Four components are trained: a Forecaster F_1 and his surrogate F_2 , a Denoiser D , and a Classifier C . These components are then assembled at test time to form the four models. All of them are implemented using PyTorch and trained using the Adam optimizer with a batch size of 512.

All the corresponding hyperparameters can be found in Table 1. We trained F_1 for 10 epochs as in [71] and the adversarial version F_2 over 15 epochs, due to the difficulty of reaching convergence in adversarial training. The two remaining components C and D are trained over 40 epochs, a good balance to learn representations without overfitting the training noise.

5.4.2 Models. The four models are assembled and used only for inference. They are composed of one or more previously trained components, as depicted in Fig. 2. We evaluate the performance of these models.

Table 1: Hyperparameters used for components training

Parameter	Models			
	F_1	F_2	C	D
#training epochs	10	15	40	40
Training perturbation (ℓ_∞)	0	ϵ_f	ϵ_c	ϵ_d
Learning rate	0.008	0.008	0.01	0.005
Weight decay	0.2	0.2	0.02	0.1
Gamma	0.5	0.5	0.5	0.5
Scheduler step size	5	5	10	5

5.4.3 Objectives. Models engineered to be robust to noise prove their worth when applied to noisy sequences, thereby outperforming non-robust models. However, this robustness comes at a cost: when these models are applied to non-noisy sequences, their performance often declines compared to non-robust models. This presents a significant problem : if the sequences are typically non-noisy, the usage of a robust model could lead to substantial loss in accuracy.

Our objective is to maintain the performance level of a non-robust model on non-disturbed sequences, while reaping the benefits of robust models when applied to disturbed sequences.

5.4.4 Evaluation. In evaluating the models, their resistance to the PGD attack is assessed by comparing their performance on clean data and perturbed data, and serves as a measure of the models' robustness against adversarial perturbations.

To explore the models' resistance to different levels of perturbations, we vary two parameters: the number of perturbed steps, denoted as k , and the percentage of perturbed sequences in the test set, denoted as %pseq. For k , we examine the range from 0 (no perturbation) to 3 (all steps perturbed). Regarding %pseq, we investigate four scenarios: 0% (no perturbation), 20%, 50%, and 100% perturbed sequences in the test set. These settings allow us to assess the models' performance across a spectrum of perturbation levels, ranging from zero disturbance with normal data up to the entirety of the testing set being disturbed.

During the evaluation, we examine the impact of varying the ϵ -norm values in the triplet $(\epsilon_c, \epsilon_f, \epsilon_t)$ by setting $\epsilon_d = \epsilon_f$. Specifically, we observe how the models react when the testing phase's ϵ -norm value, ϵ_t , differs from the values of ϵ_c and ϵ_f .

Through this evaluation, we aim to demonstrate that there is a distinct advantage in decoupling ϵ_c and ϵ_f during training. Furthermore, we aim to show that a smaller ϵ_c allows the classifier to segregate data with $\epsilon_t \geq \epsilon_c$ during inference. Similarly, we seek to illustrate that a larger ϵ_f exhibits resilience at inference, even if $\epsilon_t \leq \epsilon_f$.

5.5 Results

We compared a baseline model M_1 , a robust baseline model M_2 , and two hybrid variants M_3 and M_4 (our defense mechanisms) as shown in Fig. 2. The first variant M_3 is a model that adds two extra components: the classifier C and the denoiser D . If the classifier predicts a sequence is noisy, the denoiser is used to remove the noise, and the non-robust forecaster F_1 is subsequently applied. If no disturbance is detected, F_1 is applied directly. The second

Table 2: Classifier accuracy on the test data without perturbation ($\epsilon_t = 0$) under two training conditions (ϵ_c, ϵ_f).

$(\epsilon_c, \epsilon_f) = (0.3, 0.3)$	$(\epsilon_c, \epsilon_f) = (0.2, 0.3)$
60.93%	61.23%

Table 3: Performance of the four models on the test data without perturbation ($\epsilon_t = 0$) under two training conditions (ϵ_c, ϵ_f).

Model	MSE	
	$(\epsilon_c, \epsilon_f) = (0.3, 0.3)$	$(\epsilon_c, \epsilon_f) = (0.2, 0.3)$
M1	0.0173	0.0173
M2	0.0509	0.0509
M3	0.0190	0.0188
M4	0.0257	0.0234

variant M_4 involves the classifier that predicts whether a sequence is disturbed. If a disturbance is detected, the robust forecaster F_2 is applied; otherwise, F_1 is used.

We select 100 base stations to predict call volume in Milan, incorporating data points from 1 hour, 2 hours, and 24 hours prior to the prediction, testing hourly for a week following a 7-week training period. The results in the tables represent the average MSE across all base stations for the test week. All results presented are from the testing phase.

Both F_2 and D were trained with a disturbance norm $\epsilon_f = \epsilon_d = 0.3$ throughout the training process. However, the training norm ϵ_c for C is varied from 0.2 to 0.3, and we also observe test results with different norms ϵ_t from 0.1 to 0.4.

5.5.1 Clean data with $\epsilon_c = \epsilon_f$. The results presented in Table 3 demonstrate a significant improvement in the effectiveness of M_3 and M_4 , particularly when there is no poisoning involved, compared to M_2 [41]. Specifically, while the robust M_2 model experiences an MSE multiplied by a factor of 2.94 (from 0.0173 to 0.0509) on non-poisoned sequences, M_3 and M_4 manage to maintain a performance almost equivalent to that of model M_1 with an MSE increasing only by a factor of 1.1 and 1.49 respectively.

Table 2 shows the classifier's accuracy on normal samples. 60.93% of the normal sequences are correctly classified, thus 39.07% of are incorrectly predicted as perturbed. This high false positive rate is likely due to the high natural variance in the original dataset. Interestingly, with a low accuracy of 60.93%, M_3 manages to match the base MSE of model M_1 . This suggests that there is room for further improvement. In fact, out of M_3 's MSE of 0.0190, 91.1% is attributed to the base error of model M_1 , and 8.9% is due to the additional error of both the classifier and the denoiser. We can assume that if this additional error tends towards zero, then the MSE of M_3 on perturbed data would be equal to that of M_1 on normal data. This would effectively break the trade-off between robustness and accuracy.

We now turn our attention to how these models perform when faced with poisoned data.

5.5.2 Perturbed data with $\epsilon_c = \epsilon_f$. Table 5 shows the results as a function of k and %pseq. We note that our M_3 model performs significantly better than the M_2 model with an MSE up to 2.33x lower. The exception is when the whole testing set is perturbed. However, to achieve this result, we would need to assume that an attacker could perturb all 100 base stations at each time step, a scenario that is practically implausible.

We also examine the classifier's ability to detect perturbed sequences, as shown in Table 4. We observe high accuracy when k is either 1 or 2 and %pseq is either 20% or 50% but notice a decrease in accuracy in two specific scenarios. Firstly, when k increases, it becomes more challenging for the classifier to detect the poison because this trained neural network may rely on certain metrics, such as the difference in values between two points or the standard deviation whereas if $k = 3$, most of the sequences simply shifts in level, making the detection more complicated. The second scenario is when $\epsilon_t \leq \epsilon_c$, as it is more difficult for the model to separate noisy and normal sequences with a smaller ϵ_t .

Given these observations, we plan to test a new scenario by decoupling ϵ_c and ϵ_f , specifically, setting ϵ_c to be less than ϵ_f .

5.5.3 Clean data with $\epsilon_c < \epsilon_f$. We first observe that decoupling ϵ_c and ϵ_f slightly improves performance. More than the raw results of accuracy or MSE, we are interested in their correlation when ϵ_c goes from 0.3 to 0.2. We notice that a 0.5% increase in classifier accuracy corresponds to a 1.1% decrease in M_3 's MSE and an 8.9% decrease in M_4 's MSE. Given that the base error of the model is 0.0173, the relationship between accuracy increase and MSE decrease is likely non-linear, with the MSE's decrease diminishing as accuracy becomes very high. This correlation is noteworthy, and the precise relationship between accuracy's increase and MSE's decrease in this context could be a subject for future research. In comparison to the clean data when $\epsilon_c = \epsilon_f$, M_3 recovers 92.02% of the baseline error from M_1 , with an MSE 2.71x lower than M_2 . M_4 is now recovering 73.93% of M_1 's error, representing an increase of 6.61% compared to the previous scenario.

5.5.4 Perturbed data with $\epsilon_c < \epsilon_f$ and $\epsilon_t \leq \epsilon_f$. We examine results for $\epsilon_c = 0.2$, $\epsilon_f = 0.3$, and ϵ_t values varying from 0.10, to 0.30. In most of the scenarios, M_3 performs best. Several observations can be made from the results. Firstly, without adversarial training, M_1 's MSE significantly increases when facing perturbations. Secondly, M_2 's MSE experiences the smallest increase, but this MSE is much higher compared to M_3 and M_4 . Finally, we note that the benefit of robust models becomes limited when ϵ_t is very small. In this scenario, M_1 gains ground on the others, suggesting adversarial training is beneficial when $\epsilon_t \geq 0.1$. M_2 is suitable for extreme cases where the entire test can be perturbed with very large ϵ_t , exceeding 0.3, which is challenging in practice. Therefore, we prefer the use of M_3 .

Finally, regarding the classifier, we aim to address our hypothesis: if a classifier is trained to detect adversarial examples with ϵ_c , does this imply it can detect them with ϵ_t greater than ϵ_c ? The answer is yes, except for the unique case of a shift of the whole sequence for $k = 3$. Lastly, we also observe that as ϵ_t becomes small, it becomes increasingly challenging for the classifier to separate the data.

5.5.5 *Perturbed data with $\epsilon_c < \epsilon_f$ and $\epsilon_t > \epsilon_f$.* Finally, when ϵ_t is larger than ϵ_c and ϵ_f , model M_4 appears to be a good compromise for $k = 2$ and $\%pseq \leq 50\%$. For $k = 3$ and $\%pseq \geq 50\%$, we would prefer model M_2 with adversarial training. However, we can assume that in such a case, experts could easily detect perturbations with $\epsilon_t = 0.4$ on all the historical data steps for each of the 100 base stations.

For the classification task, the performance is quite similar to (0.2, 0.3, 0.3).

5.6 Discussion and Comparison

One of our key findings is the potential of model M_3 , composed of 3 components: a classifier to detect the poisoned samples, a denoiser to remove the noise from them, and a forecaster trained on normal samples only. Specifically, M_3 performed $2.71\times$ better than M_2 , retaining 92.02% of M_1 's MSE on normal data, while maintaining performance on perturbed data that was up to $1.71\times$ lower than M_1 , especially in the cases of high perturbation, and $2.51\times$ lower than M_2 , particularly in the cases of low perturbation. We therefore postulate that if the classifier approaches an accuracy near 100% and the denoiser's MSE approaches 0, the performance of M_3 on perturbed data would align with the performance of the standard model M_1 on clean data. This effectively breaks the traditional trade-off between robustness and accuracy.

Furthermore, our results confirmed that a classifier trained to detect adversarial examples with a certain ϵ_c -norm value can detect them if $\epsilon_t \geq \epsilon_c$ at test time, except when all the steps in historical data are perturbed. The results showed significant difference from the ones reported in [71], which employed an LSTM-based methodology for predicting call volume, while the performance was reduced down to 72.39% of the original model's performance if defense mechanism was incorporated. This resulted in an MSE of 0.0902, marking an increase of $1.38\times$ from their original MSE value of 0.0653. On the other hand, our M_3 showcased enhanced resilience, maintaining 92.02% of the baseline performance after defense, resulting in an MSE rising only by a factor of 1.09. The comparative evaluation underscores the efficiency of our models (especially of M_3) on mitigating the ramifications of adversarial attacks, and safeguarding the fidelity of time series forecasting.

6 CONCLUSION

In this paper, we addressed the long-standing challenge about simultaneously achieving performance and robustness of deep forecasting models in the face of poisoning attacks. We systematically investigated the strengths and weaknesses of each model under different scenarios by varying the perturbation levels and ϵ -norm values, and studied the complementary roles of adversarial training, adversarial examples classification, and denoising in enhancing model robustness.

We took wireless traffic prediction as a specific scenario and developed a new type of attack where an attacker can perturb any subsequence step of any base station with a 10-steps PGD attack on clean forecaster F_1 . We then proposed two defense mechanisms by assembling adversarially (versus cleanly) trained forecaster, classifier, and denoiser, with the objective to maintain performance on normal data while preserving robustness to poisoned data. By theoretically and experimentally demonstrating the possibility of breaking the trade-off between model robustness and accuracy, we believe that our findings laid down a foundation for further development of robust and reliable deep forecasting models, which therefore deserve more attention and effort from the community.

Table 4: Classifier accuracy (in %) based on the percentage of perturbed sequences (%pseq) and the number of perturbed steps k for different values of poison levels for classifier (ϵ_c) and forecaster (ϵ_f) in training and testing (ϵ_t).

%pseq	Classifier accuracy at different $(\epsilon_c, \epsilon_f, \epsilon_t)$									(0.3, 0.3, 0.3)			(0.3, 0.2)			(0.2, 0.3, 0.3)			(0.2, 0.3, 0.2)			(0.2, 0.3, 0.15)			(0.2, 0.3, 0.1)			(0.2, 0.3, 0.4)		
	$k = 1$	$k = 2$	$k = 3$	$k = 1$	$k = 2$	$k = 3$	$k = 1$	$k = 2$	$k = 3$	$k = 1$	$k = 2$	$k = 3$	$k = 1$	$k = 2$	$k = 3$	$k = 1$	$k = 2$	$k = 3$	$k = 1$	$k = 2$	$k = 3$									
	20	80.78	79.28	58.75	76.12	75.14	62.32	77.42	75.61	55.98	74.81	73.83	64.27	72.42	72.10	65.07	69.03	69.17	60.34	78.32	75.88	51.68								
50	86.64	83.85	60.48	82.70	80.31	51.42	82.62	80.68	61.26	80.31	79.33	66.88	77.35	77.11	62.49	71.35	72.48	54.49	83.02	80.16	44.74									
100	70.52	67.64	31.70	66.47	62.58	33.97	67.64	68.99	56.51	64.15	65.01	41.29	60.82	58.44	39.34	54.39	49.78	39.60	69.15	70.39	54.62									

Table 5: Performance of the four models at different values of the percentages of perturbed sequences (%pseq), the number of perturbed steps k , and the poison levels for classifier (ϵ_c) and forecaster (ϵ_f) in training and testing (ϵ_t).

%pseq Model	MSE at different $(\epsilon_c, \epsilon_f, \epsilon_t)$									(0.3, 0.3, 0.3)			(0.3, 0.2)			(0.2, 0.3, 0.3)			(0.2, 0.3, 0.2)			(0.2, 0.3, 0.15)			(0.2, 0.3, 0.1)			(0.2, 0.3, 0.4)																																																																																
	$k = 1$	$k = 2$	$k = 3$	$k = 1$	$k = 2$	$k = 3$	$k = 1$	$k = 2$	$k = 3$	$k = 1$	$k = 2$	$k = 3$	$k = 1$	$k = 2$	$k = 3$	$k = 1$	$k = 2$	$k = 3$	$k = 1$	$k = 2$	$k = 3$																																																																																							
	20	M1 0.0212 0.0276 0.0367 0.0196 0.0229 0.0273 0.0276 0.0367 0.0196 0.0229 0.0273 0.0189 0.0211 0.0238 0.0183 0.0195 0.0210 0.0232 0.0333 0.0483	M2	0.0513	0.0518	0.0523	0.0515	0.0518	0.0523	0.0512	0.0515	0.0518	0.0512	0.0514	0.0516	0.0511	0.0512	0.0514	0.0515	0.0521	0.0528	M3	0.0251	0.0279 0.0343 0.0220 0.0236 0.0264 0.0251 0.0276 0.0347 0.0216 0.0232 0.0259 0.0206 0.0216 0.0236 0.0199 0.0204 0.0216 0.0286 0.0331 0.0468	M4	0.0260	0.0278 0.0391 0.0270 0.0282 0.0333 0.0259 0.0277 0.0374 0.0259 0.0273 0.0316 0.0262 0.0273 0.0298 0.0262 0.0271 0.0263 0.0261 0.0283 0.0493	M1	0.0272	0.0433	0.0662	0.0231 0.0315 0.0426 0.0272 0.0434 0.0662 0.0231 0.0316 0.0427 0.0214 0.0269 0.0338 0.0198 0.0230 0.0267 0.0321 0.0580 0.0958	M2	0.0520	0.0532	0.0544	0.0517	0.0532	0.0544	0.0517	0.0524	0.0532	0.0515	0.0521	0.0526	0.0513	0.0517	0.0521	0.0524	0.0540	0.0557	M3	0.0311	0.0377 0.0523 0.0258 0.0292 0.0381 0.0312 0.0377 0.0507 0.0253 0.0291 0.0358 0.0231 0.0256 0.0303 0.0214 0.0229 0.0259 0.0371 0.0474 0.0840	M4	0.0348	0.0388	0.0578	0.0338	0.0368	0.0526	0.0350	0.0350	0.0391	0.0559	0.0333	0.0366	0.0447	0.0325	0.0353	0.0379	0.0311	0.0334	0.0302	0.0416 0.0821	M1	0.0371	0.0689	0.1147	0.0289 0.0454 0.0675 0.0372 0.0690 0.1145 0.0290 0.0456 0.0678 0.0254 0.0362 0.0499 0.0224 0.0286 0.0360 0.0468 0.0984 0.1737	M2	0.0531	0.0555	0.0579 0.0524 0.0540 0.0555 0.0532 0.0559 0.0524 0.0540 0.0555 0.0520 0.0532 0.0544 0.0517 0.0524 0.0532 0.0539 0.0571 0.0605	M3	0.0390	0.0496 0.0958 0.0311 0.0379 0.0582 0.0395 0.0495 0.0760 0.0308 0.0382 0.0553 0.0271 0.0325 0.0429 0.0238 0.0271 0.0327 0.0494 0.0612 0.1014	M4	0.0510	0.0613	0.0920	0.0449	0.0523	0.0579	0.0505	0.0643	0.0889	0.0438	0.0527	0.0600	0.0400	0.0455	0.0464	0.0346	0.0519	0.0360	0.0576	0.0689

REFERENCES

[1] Sheila Alemany and Niki Pissinou. 2022. The Dilemma Between Data Transformations and Adversarial Robustness for Time Series Application Systems. In *Proceedings of the Workshop on Artificial Intelligence Safety 2022 (SafeAI 2022) co-located with the Thirty-Sixth AAAI Conference on Artificial Intelligence (AAAI2022), Virtual, February, 2022 (CEUR Workshop Proceedings)*, Gabriel Pedroza, José Hernández-Orallo, Xin Cynthia Chen, Xiaowei Huang, Huáscar Espinoza, Mauricio Castillo-Effen, John A. McDermid, Richard Mallah, and Seán Ó hEigearaigh (Eds.), Vol. 3087. CEUR-WS.org, Virtual Conference, 1–8.

[2] Youness Arjoune and Saleh Faruque. 2020. Artificial Intelligence for 5G Wireless Systems: Opportunities, Challenges, and Future Research Direction. In *2020 10th Annual Computing and Communication Workshop and Conference (CCWC)*. IEEE, Las Vegas, NV, USA, 1023–1028. <https://doi.org/10.1109/CCWC47524.2020.9031117>

[3] Shaojie Bai, J Zico Kolter, and Vladlen Koltun. 2018. An empirical evaluation of generic convolutional and recurrent networks for sequence modeling. *arXiv preprint arXiv:1803.01271* (2018).

[4] Gianni Barlačchi, Marco De Nadai, Roberto Larcher, Antonio Casella, Cristiana Chitic, Giovanni Torrisi, Fabrizio Antonelli, Alessandro Vespignani, Alex Pentland, and Bruno Lepri. 2015. A multi-source dataset of urban life in the city of Milan and the Province of Trentino. *Scientific Data* 2, 1 (Oct. 2015), 150055.

[5] Marco Barreno, Blaine Nelson, Russell Sears, Anthony D Joseph, and J D Tygar. 2006. Can machine learning be secure? *Proceedings of the 2006 ACM Symposium on Information, Computer and Communications Security* (2006), 16–25.

[6] Battista Biggio, Giorgio Fumera, and Fabio Roli. 2014. Security evaluation of pattern classifiers under attack. *IEEE Transactions on Knowledge and Data Engineering* 26, 4 (2014), 984–996.

[7] Battista Biggio, Blaine Nelson, and Pavel Laskov. 2013. Poisoning Attacks against Support Vector Machines. *arXiv:1206.6389 [cs.LG]*

[8] Anastasia Borovykh, Sander Bohte, and Cornelis W Oosterlee. 2017. Conditional time series forecasting with convolutional neural networks. *arXiv preprint arXiv:1703.04691* (2017).

[9] Alessio Botta, Walter de Donato, Valerio Persico, and Antonio Pescapé. 2016. Integration of Cloud computing and Internet of Things: A survey. *Future Generation Computer Systems* 56 (2016), 684–700. <https://doi.org/10.1016/j.future.2015.09.021>

[10] George EP Box and Gwilym M Jenkins. 1976. *Time series analysis: forecasting and control*. Holden-Day San Francisco.

[11] Oliver Bryniarski, Nabeel Hingun, Pedro Pachuca, Vincent Wang, and Nicholas Carlini. 2021. Evading Adversarial Example Detection Defenses with Orthogonal Projected Gradient Descent. *ArXiv abs/2106.15023* (2021).

[12] C. Yang C. Yao and I. Chih-Lin. 2017. Data-Driven Resource Allocation with Traffic Load Prediction. *Journal of Communications and Information Networks* 2, 1 (2017), 52–65. <https://doi.org/10.1007/s41650-017-0005-y>

[13] Nicholas Carlini and David Wagner. 2017. MagNet and "Efficient Defenses Against Adversarial Attacks" are Not Robust to Adversarial Examples. *arXiv:1711.08478 [cs.LG]*

[14] Ferhat Ozgur Catak, Murat Kuzlu, Evren Catak, Umit Cali, and Ozgur Guler. 2022. Defensive Distillation-Based Adversarial Attack Mitigation Method for Channel Estimation Using Deep Learning Models in Next-Generation Wireless Networks. *IEEE Access* (2022). <https://doi.org/10.1109/access.2022.3206385>

[15] Chris Chatfield. 2003. *The analysis of time series: an introduction*. CRC Press.

[16] Pin-Yu Chen, Huan Zhang, Yash Sharma, Jinfeng Yi, and Cho-Jui Hsieh. 2017. Zoo: Zeroth order optimization based black-box attacks to deep neural networks without training substitute models. In *Proceedings of the 10th ACM Workshop on Artificial Intelligence and Security*, 15–26.

[17] Xinyun Chen, Chang Liu, Bo Li, Kimberly Lu, and Dawn Song. 2017. Targeted Backdoor Attacks on Deep Learning Systems Using Data Poisoning. *arXiv:1712.05526 [cs.CR]*

[18] Kyunghyun Cho, Bart Van Merriënboer, Caglar Gulcehre, Dzmitry Bahdanau, Fethi Bougares, Holger Schwenk, and Yoshua Bengio. 2014. Learning phrase representations using RNN encoder-decoder for statistical machine translation. *arXiv preprint arXiv:1406.1078* (2014).

[19] Edward Choi, Mohammad Taha Bahadori, Andy Schuetz, Walter F Stewart, and Jimeng Sun. 2016. Doctor AI: Predicting clinical events via recurrent neural networks. In *Machine Learning for Healthcare Conference*. PMLR, 301–318.

[20] Robert B Cleveland, William S Cleveland, Jean E McRae, and Irma Terpenning. 1990. STL: A seasonal-trend decomposition procedure based on loess. *Journal of Official Statistics* 6, 1 (1990), 3–73.

[21] Yaping Cui, Xinyun Huang, Dapeng Wu, and Hao Zheng. 2020. Machine Learning-Based Resource Allocation Strategy for Network Slicing in Vehicular Networks. *Wireless Communications and Mobile Computing* (2020). <https://doi.org/10.1155/2020/883615>

[22] Yinpeng Dong, Fangzhou Liao, Tianyu Pang, Hang Su, Jun Zhu, Xiaolin Hu, and Jianguo Li. 2018. Boosting Adversarial Attacks with Momentum. In *Proceedings of the IEEE Conference on Computer Vision and Pattern Recognition*.

[23] John C. Duchi, Peter L. Bartlett, and Martin J. Wainwright. 2012. Randomized Smoothing for Stochastic Optimization. *SIAM Journal on Optimization* 22, 2 (2012), 674–701. <https://doi.org/10.1137/110831659>

[24] Ian J. Goodfellow, Jonathon Shlens, and Christian Szegedy. 2015. Explaining and Harnessing Adversarial Examples. *arXiv:1412.6572 [stat.ML]*

[25] Yuvaraj Govindarajulu, Avinash Ambalal, Pavan Kulkarni, and Manojkumar Parmar. 2023. Targeted Attacks on Timeseries Forecasting. *arXiv:2301.11544 [cs.LG]*

[26] Sven Gowal, Chongli Qin, Jonathan Uesato, Timothy Mann, and Pushmeet Kohli. 2020. Uncovering the Limits of Adversarial Training against Norm-Bounded Adversarial Examples. *arXiv:2010.03593 [stat.ML]*

[27] David Hallac, Suvrit Vare, Stephen Boyd, and Jure Leskovec. 2017. Toeplitz Inverse Covariance-Based Clustering of Multivariate Time Series Data. In *Proceedings of the 23rd ACM SIGKDD International Conference on Knowledge Discovery and Data Mining*, 215–223.

[28] James D Hamilton. 1994. *Time series analysis*. Princeton university press.

[29] Sepp Hochreiter and Jürgen Schmidhuber. 1997. Long short-term memory. *Neural computation* 9, 8 (1997), 1735–1780.

[30] Tao Hong, Pierre Pinson, and Shu Fan. 2014. Global energy forecasting competition 2012. *International Journal of Forecasting* 30, 2 (2014), 357 – 363. <https://doi.org/10.1016/j.ijforecast.2013.07.001>

[31] Rob J Hyndman and George Athanasopoulos. 2018. *Forecasting: principles and practice*. OTexts.

[32] Rob J Hyndman, Anne B Koehler, J Keith Ord, and Ralph D Snyder. 2008. *Forecasting with exponential smoothing: the state space approach*. Springer Science & Business Media.

[33] Robin Jia and Percy Liang. 2017. Adversarial examples for evaluating reading comprehension systems. In *Proceedings of the 2017 Conference on Empirical Methods in Natural Language Processing*, 2021–2031.

[34] Fazle Karim, Somshubra Majumdar, and Houshang Darabi. 2021. Adversarial Attacks on Time Series. *IEEE Transactions on Pattern Analysis and Machine Intelligence* 43, 10 (2021), 3309–3320. <https://doi.org/10.1109/TPAMI.2020.2986319>

[35] Alexey Kurakin, Ian J Goodfellow, and Samy Bengio. 2016. Adversarial examples in the physical world. In *Workshop on Adversarial Training at the 30th International Conference on Neural Information Processing Systems*.

[36] Bo Li and Yevgeniy Vorobeychik. 2015. Data poisoning attacks on factorization-based collaborative filtering. In *Advances in Neural Information Processing Systems*, 1885–1893.

[37] Bryan Lim, Stefan Zohren, and Stephen Roberts. 2020. Temporal fusion transformers for interpretable multi-horizon time series forecasting. *arXiv preprint arXiv:1912.09363* (2020).

[38] Fan Liu, Hao Liu, and Wenzhao Jiang. 2022. Practical Adversarial Attacks on Spatiotemporal Traffic Forecasting Models. *arXiv:2210.02447 [cs.LG]*

[39] Linbo Liu, Younghun Park, Trong Nghia Hoang, Hilaf Hasson, and Jun Huan. 2023. Robust Multivariate Time-Series Forecasting: Adversarial Attacks and Defense Mechanisms. *ICLR* (2023). <https://arxiv.org/abs/2207.09572v1>

[40] Yingqi Liu, Shiqing Ma, Yousa Afar, Wen-Chuan Lee, Jianhai Zhai, Weihang Wang, and Xiangyu Zhang. 2017. Trojaning attack on neural networks. *arXiv preprint arXiv:1802.03043* (2017).

[41] Aleksander Madry, Aleksandar Makelov, Ludwig Schmidt, Dimitris Tsipras, and Adrian Vladu. 2018. Towards deep learning models resistant to adversarial attacks. In *International Conference on Learning Representations*.

[42] Shike Mei and Xiaojin Zhu. 2015. Using machine teaching to identify optimal training-set attacks on machine learners. In *Twenty-Ninth AAAI Conference on Artificial Intelligence*.

[43] Michael Mosbach, Maksym Andriushchenko, Thomas Trost, Matthias Hein, and Dietrich Klakow. 2018. Logit Pairing Methods Can Fool Gradient-Based Attacks. *arXiv preprint arXiv:1810.12042* (2018).

[44] Manfred Mudelsee. 2019. Trend analysis of climate time series: A review of methods. *Earth-Science Reviews* 190 (2019), 310–322. <https://doi.org/10.1016/j.earscirev.2018.12.005>

[45] Mohsin Munir, Shoaib Ahmed Siddiqui, Andreas Dengel, and Sheraz Ahmed. 2019. DeepAnT: A Deep Learning Approach for Unsupervised Anomaly Detection in Time Series. *IEEE Access* 7 (2019), 1991–2005. <https://doi.org/10.1109/ACCESS.2018.2886457>

[46] Roi Naveiro. 2021. Adversarial attacks against Bayesian forecasting dynamic models. *arXiv preprint arXiv:2110.10783* (2021).

[47] Nicolas Papernot, Patrick McDaniel, and Ian Goodfellow. 2015. Transferability in machine learning: from phenomena to black-box attacks using adversarial samples. *arXiv preprint arXiv:1605.07277* (2015).

[48] Nicolas Papernot, Patrick McDaniel, Ian Goodfellow, Somesh Jha, Z. Berkay Celik, and Ananthram Swami. 2016. Practical black-box attacks against machine learning. In *Proceedings of the 2017 ACM on Asia Conference on Computer and Communications Security*, 506–519.

[49] Nicolas Papernot, Patrick McDaniel, Somesh Jha, Matt Fredrikson, Z. Berkay Celik, and Ananthram Swami. 2015. The Limitations of Deep Learning in Adversarial Settings. *arXiv:1511.07528 [cs.CR]*

[50] Syama Sundar Rangapuram, Matthias W Seeger, Jan Gasthaus, Lorenzo Stella, Yuyang Wang, and Tim Januschowski. 2018. Deep state space models for time series forecasting. *Advances in Neural Information Processing Systems* 31 (2018).

[51] Benjamin I.P. Rubinstein, Blaine Nelson, Ling Huang, Anthony D. Joseph, Shing-hon Lau, Satish Rao, Nina Taft, and J. D. Tygar. 2009. ANTIDOTE: Understanding and Defending against Poisoning of Anomaly Detectors. In *Proceedings of the 9th ACM SIGCOMM Conference on Internet Measurement (Chicago, Illinois, USA) (IMC '09)*. Association for Computing Machinery, New York, NY, USA, 1–14. <https://doi.org/10.1145/1644893.1644895>

[52] J. J. Lehtomäki S. P. Sone and Z. Khan. 2020. Wireless Traffic Usage Forecasting Using Real Enterprise Network Data: Analysis and Methods. *IEEE Open Journal of the Communications Society* 1 (2020), 777–797. <https://ieeexplore.ieee.org/document/9108216>

[53] David Salinas, Valentin Flunkert, Jan Gasthaus, and Tim Januschowski. 2020. DeepAR: Probabilistic forecasting with autoregressive recurrent networks. *International Journal of Forecasting* 36, 3 (2020), 1181–1191.

[54] Arawinkuma Selvakkumar, Shantanu Pal, and Zahra Jadidi. 2021. Addressing Adversarial Machine Learning Attacks in Smart Healthcare Perspectives. *CoRR* abs/2112.08862 (2021). arXiv:2112.08862

[55] Ali Shafahi, Amin Ghiasi, Furong Huang, and Tom Goldstein. 2019. Label Smoothing and Logit Squeezing: A Replacement for Adversarial Training? *arXiv preprint arXiv:1910.11585* (2019).

[56] Robert H Shumway and David S Stoffer. 2017. *Time series analysis and its applications: with R examples*. Springer.

[57] Jacob Steinhardt, Pang Wei Koh, and Percy Liang. 2017. Certified defenses for data poisoning attacks. In *Advances in Neural Information Processing Systems*. 3517–3529.

[58] Christian Szegedy, Wojciech Zaremba, Ilya Sutskever, Joan Bruna, Dumitru Erhan, Ian Goodfellow, and Rob Fergus. 2014. Intriguing properties of neural networks. arXiv:1312.6199 [cs.CV]

[59] M.J. Teixeira and V.S. Timóteo. 2021. A Predictive Resource Allocation for Wireless Communications Systems. *SN COMPUT. SCI* (2021). <https://doi.org/10.1007/s42979-021-00854-8>

[60] Florian Tramer. 2022. Detecting Adversarial Examples Is (Nearly) As Hard As Classifying Them. In *Proceedings of the 39th International Conference on Machine Learning (Proceedings of Machine Learning Research)*, Vol. 162. PMLR, 21692–21702. <https://proceedings.mlr.press/v162/tramer22a.html>

[61] Ashish Vaswani, Noam Shazeer, Niki Parmar, Jakob Uszkoreit, Llion Jones, Aidan N Gomez, Łukasz Kaiser, and Illia Polosukhin. 2017. Attention is All you Need. In *Advances in Neural Information Processing Systems*, I. Guyon, U. Von Luxburg, S. Bengio, H. Wallach, R. Fergus, S. Vishwanathan, and R. Garnett (Eds.), Vol. 30. Curran Associates, Inc.

[62] Yuyang Wang, Alex Smola, Danielle Maddix, Jan Gasthaus, Dean Foster, and Tim Januschowski. 2019. Deep factors for forecasting. *arXiv preprint arXiv:1905.12417* (2019).

[63] Shixian Wen and Laurent Itti. 2019. Adversarial Training: embedding adversarial perturbations into the parameter space of a neural network to build a robust system. *arXiv preprint arXiv:1910.04279* (2019).

[64] H. Gao X. Xing, Y. Lin and Y. Lu. 2021. Wireless Traffic Prediction with Series Fluctuation Pattern Clustering. *IEEE International Conference on Communications Workshops (ICC Workshops)* (2021), 1–6. <https://doi.org/10.1109/ICCWorkshops50388.2021.9473514>

[65] Huang Xiao, Battista Biggio, Gavin Brown, Giorgio Fumera, Claire Eckert, and Fabio Roli. 2015. Is feature selection secure against training data poisoning?. In *International Conference on Machine Learning*. 1689–1698.

[66] Cihang Xie, Yuxin Wu, Laurens van der Maaten, Alan Yuille, and Kaiming He. 2019. Feature Denoising for Improving Adversarial Robustness. arXiv:1812.03411 [cs.CV]

[67] Fuxun Yu, Qide Dong, and Xiang Chen. 2018. ASP: A Fast Adversarial Attack Example Generation Framework based on Adversarial Saliency Prediction. *arXiv preprint arXiv:1802.05763* (2018).

[68] Guowei Zhang, Paul Patras, and Hamed Haddadi. 2019. Deep learning in mobile and wireless networking: A survey. *IEEE Communications Surveys & Tutorials* 21, 3 (2019), 2224–2287.

[69] Hongyang Zhang, Yaodong Yu, Jiantao Jiao, Eric P. Xing, Laurent El Ghaoui, and Michael I. Jordan. 2019. Theoretically Principled Trade-off between Robustness and Accuracy. arXiv:1901.08573 [cs.LG]

[70] Jingfeng Zhang, Xilie Xu, Bo Han, Gang Niu, Lizhen Cui, Masashi Sugiyama, and Mohan Kankanhalli. 2020. Attacks Which Do Not Kill Training Make Adversarial Learning Stronger. *ArXiv* abs/2002.11242 (2020).

[71] Tianhang Zheng and Baochun Li. 2022. Poisoning Attacks on Deep Learning based Wireless Traffic Prediction. In *IEEE INFOCOM 2022 - IEEE Conference on Computer Communications*. IEEE, London, United Kingdom, 660–669. <https://doi.org/10.1109/INFOCOM48880.2022.9796791>

[72] Xiaojin Zhu. 2018. An Optimal Control View of Adversarial Machine Learning. *arXiv preprint arXiv:1811.04422* (2018).